Published in final edited form as:

J Am Chem Soc. 2019 February 06; 141(5): 1867–1870. doi:10.1021/jacs.8b12670.

Formation of a Reactive, Alkyl Thiolate-Ligated Fe^{III}-Superoxo Intermediate Derived from Dioxygen

Maike N. Blakely, **Maksym A. Dedushko**, **Penny Chaau Yan Poon**, **Gloria Villar-Acevedo**, **Julie A. Kovacs***

Department of Chemistry, University of Washington, Campus Box 351700, Seattle, Washington 98195, United States

Abstract

Herein, we describe an alkyl thiolate-ligated iron complex that reacts with dioxygen to form an unprecedented example of an iron superoxo ($O_2^{\bullet-}$) intermediate, [$Fe^{III}(S_2^{Me2}N_3$(Pr,Pr))(O_2)] (**4**), which is capable of cleaving strong C–H bonds. A cysteinate-ligated iron superoxo intermediate is proposed to play a key role in the biosynthesis of β-lactam antibiotics by isopenicillin N-synthase (IPNS). Superoxo **4** converts to a metastable putative Fe(III)–OOH intermediate, at rates that are dependent on the C–H bond strength of the H atom donor, with a kinetic isotope effect (k_H/k_D = 4.8) comparable to that of IPNS (k_H/k_D = 5.6). The bond dissociation energy of the C–H bonds cleaved by **4** (92 kcal/mol) is comparable to C–H bonds cleaved by IPNS (93 kcal/mol). Both the calculated and experimental electronic absorption spectra of **4** are comparable to those of the putative IPNS superoxo intermediate, and are shown to involve $RS^- \rightarrow Fe–O_2^{\bullet-}$ and $O_2^{\bullet-} \rightarrow Fe$ charge transfer transitions. The π-back-donation by the electronrich alkyl thiolate presumably facilitates this reactivity by increasing the basicity of the distal oxygen. The frontier orbitals of **4** are shown to consist of two strongly coupled unpaired electrons of opposite spin, one in a superoxo π^*(O–O) orbital, and the other in an Fe(d_{xy}) orbital.

Isopenicillin N synthase (IPNS)[1–4] and cysteine dioxygenase (CDO)[5–10] are nonheme Fe enzymes that catalyze the O_2-promoted oxidation of cysteinates (RS^-). Although O_2 oxidation reactions are thermodynamically favored, they are kinetically slow in the absence of a transition-metal catalyst, because they are spin-forbidden.[11] The electron donor properties of cysteinate and high covalency of Fe^{III}–SR bonds[12,13] lower the activation barrier to O_2 binding[4] to iron, promote O–O bond cleavage,[4,14] and increase the reactivity of high-valent Fe-oxo intermediates.[15,16] This helps to facilitate the oxidative bicyclization reaction involved in the biosynthesis of β-lactam antibiotics (e.g., penicillin, cephalosporins)

*Corresponding Author kovacs@uw.edu.

ASSOCIATED CONTENT

Supporting Information

The Supporting Information is available free of charge on the ACS Publications website at DOI: 10.1021/jacs.8b12670. Experimental Section, crystallographic tables for **1**; quantitative UV/vis of **1**; ESI-MS of **3** (generated from **1**+$^{18}O_2$), and **4**; LT ^{1}H NMR of the reaction **1**+O_2; rR spectrum of **1**, **3**, and **4** generated from $^{16}O_2$ and $^{18}O_2$; electronic absorption spectrum of **2**+KO_2, putative Fe^{III}–OOH **5**, and its conversion to **3**; DFT optimized structure of **4**; TD-DFT calculated vs experimental electronic absorption spectrum of **4**; calibration curve used for spin quantitation of EPR spectra (PDF)

The authors declare no competing financial interest.

by IPNS,[1,3] as well as the CDO-catalyzed regulation of cysteine concentration, toxic levels of which can lead to neurological disorders,[17] or the metastasis of cancerous tumors.[18,19] The proposed mechanism of both IPNS[2,3] and CDO[5,6] involves the initial formation of a *cis* thiolate-ligated iron superoxo intermediate (*cis*-RS-Fe-$O_2^{\bullet-}$). With the former, this intermediate abstracts a H atom from substrate, and with the latter it is proposed to attack the adjacent sulfur to form a transient peroxythiolate species. The putative IPNS Fe–$O_2^{\bullet-}$ is spectroscopically detected in small amounts (14%) via transient absorption (λ_{max} = 630 nm; t = 2–10 ms) and Mössbauer spectroscopies if the cysteinate β-hydrogens are deuterated.[2] A CDO intermediate, proposed to be an Fe(III)-peroxythiolate, is also observed by transient absorption spectroscopy (λ_{max} = 500 nm, 640 nm).[5] Vibrational data is not available to support these assignments, however. Two strong C–H bonds are cleaved during the proposed IPNS mechanism (Figure S1): a β-hydrogen from cysteine (93 kcal/mol) and a β-hydrogen from valine (96 kcal/mol).[20] The former is proposed to involve the putative Fe(III)-superoxo, and the latter an Fe(IV)-oxo intermediate.[2] There are few well-characterized examples of Fe(III)-superoxo compounds,[21–24] however, and none of these cleave strong C–H bonds. An aryl thiolate-ligated Fe–$O_2^{\bullet-}$ was recently reported; however, the sulfur lone pair is tied up in π-bonding to the aryl carbon in one of its resonance forms making it less reactive.[23] Although it has yet to be demonstrated with a superoxo, π-back-donation by an electron rich alkyl thiolate has been shown to facilitate the cleavage of strong C–H bonds by increasing the basicity of an iron oxo.[25] Herein, we report the synthesis and structure of an alkyl thiolate-ligated iron complex that reacts with O_2 to afford a spectroscopically observable reactive intermediate.

Reduced [$Fe^{II}(S_2{}^{Me2}N_3(Pr,Pr))$] (**1**) was synthesized and structurally characterized according to the method outlined in the Supporting Information, and was shown to contain Fe^{2+} in a distorted trigonal bipyramidal coordination environment (τ = 0.78; Figure 1, Tables S2–S6). In solution, **1** has a magnetic moment of μ = 2.63 μ_B at 298 K in MeCN consistent with an S = 1 spin-state, and has a characteristic electronic absorption band at λ_{max} = 420 (ε_M 1600) nm (Figure S2). Previously, we showed that, like IPNS and CDO,[3,10,26] the oxidized derivative of **1**, [$Fe^{III}(S_2{}^{Me2}N_3(Pr,Pr))]^+$ (**2**), binds small molecules (azide and NO),[27–29] cis with respect to one of the thiolate sulfurs. The latter are frequently used to probe enzymatic O_2 binding sites.[10,14]

The addition of dry O_2 to **1** in THF at 25 °C causes an immediate color change from pale yellow to watermelon pink, with an associated shift in λ_{max} to 510(1500) nm (Figure S3), and the growth of a signal (g = 2.17, 2.11, 1.98) in the electron paramagnetic resonance (EPR) spectrum (Figure S4) consistent with the formation (in 93% yield) of low-spin (S = ½) [$Fe^{III}(\eta^2$-$S^{Me2}O)(S^{Me2}N_3(Pr,Pr))]^+$ (**3**).[30] Electrospray mass spectroscopy (ESI-MS) of isotopically labeled samples shows that the oxo of **3** is derived from $^{18}O_2$ (Figure S5). Azide inhibits this reaction (Figures S6) indicating that O_2 must bind to the metal ion in order for oxo atom transfer to occur. At low temperatures (−73 °C), a new metastable cranberry red O_2-derived intermediate, **4** (Figure 2), is observed en route to singly oxygenated **3**,[30] the low energy band (~700 nm) of which is characteristic of six-coordinate, bis-thiolate-ligated Fe(III).[12,31] When this reaction is monitored by ^{1}H NMR, the paramagnetic signals of **1** collapse to diamagnetic (S = 0) signals upon the addition of O_2 (Figure S7). The ESI-MS of

4 contains an M + 32 peak at *m/z* = 417.3 (Figure S8), consistent with the addition of two oxygen atoms to the parent ion, **1** (*m/z* = 385.4). An identical intermediate can be generated via the low temperature (−73 °C) addition of excess (50 equiv) potassium superoxide (KO_2) to oxidized $[Fe^{III}(S_2{}^{Me2}N_3(Pr,Pr))]^+$ (**2**) (Figure S9). The resonance Raman (rR) spectrum of **4** reproducibly shows isotopically sensitive features (a Fermi doublet) at 1093 and 1122 cm^{-1} (Figure 3) that shift to 1022 cm^{-1} when generated from $^{18}O_2$ (Figure S10), and disappear after 30 min, demonstrating its transient nature. All of this data would be consistent with the formation of a metastable ferric superoxo species. The calibrated (*vide infra*) density functional theory (DFT) calculated structure of $[Fe^{III}(S_2{}^{Me2}N_3(Pr,Pr))(O_2)]$ (**4**) contains an O_2 moiety *cis* to one of the thiolate sulfurs (Figure S11), with bond lengths (O–O = 1.289 Å, Table S1), and a calculated ν_{O-O} stretch (Figure S12, 1154 cm^{-1}), consistent with a ferric superoxo (Fe^{III}-$O_2^{\bullet-}$), analogous to the prop osed IPNS and CDO intermediates. The frontier orbitals of **4** (Figure 4) contain two unpaired electrons of opposite spin, one in a superoxo π^*(O–O) orbital, and the other in a Fe(d_{xy}) orbital. The calculated overlap parameter of T=0.17, and coupling constant J^{calc} = − 450 cm^{-1} indicate that the two unpaired spins are strongly coupled antiferromagnetically, consistent with the absence of paramagnetically shifted peaks in the ^{1}H NMR and EPR silence of **4**. The time-dependent DFT (TD-DFT) calculated electronic absorption spectrum of **4** (Figures S13 and S14) reproduces the experimental spectrum (Figure 2), and shows that superoxo π^*(O–O) → d_{xy}(Fe) charge transfer transitions are responsible for the higher energy bands, and a RS^- → $Fe–O_2^{\bullet-}$ charge transfer transition for the lower energy band. Both the calculated and experimental spectrum of **4** are similar to that of the putative IPNS superoxo intermediate,[2] supporting its assignment as a superoxo species. The reported CDO intermediate spectrum[5] is also similar to that of **4**, suggesting that it too is a ferric superoxo.

Ferric superoxo ($Fe^{III}–O_2^{\bullet-}$) **4** converts to a second metastable intermediate, **5** (λ_{max} = 696 nm), at −73 °C in THF (Figure S15), en route to **3** (Figure S16), at a rate that is dependent on the C–H bond strength of the solvent or H atom donor. Reaction rates decrease in deuterated THF (Figure 5), and increase upon the addition of a sacrificial H atom donor (100 equiv of 1,4-cyclohexadiene (CHD), BDE = 76 kcal/mol). The observed deuterium isotope effect, k_H/k_D = 4.8, is comparable to that of IPNS (k_H/k_D = 5.6),[32] and indicates that superoxo **4** is capable of abstracting hydrogen atoms from strong C–H bonds (BDE(THF) = 92 kcal/mol).[33] A likely product of this reaction would be a ferric hydroperoxo, $[Fe^{III}(S_2{}^{Me2}N_3(Pr,Pr))(OOH)]$ (**5**). Consistent with this, a new rhombic signal grows in when the reaction between **1** and O_2 is monitored by EPR (Figure 6). Spin-quantitation using double integration (Figure S18) indicates that the EPR signal of **5** represents 87% of the sample (Figures S4 and S17). The remaining 13% can be attributed to **1** and/or **4**, both of which are EPR-silent in ⊥-mode. Together, these results show that in contrast to the few reported Fe(III)-superoxo complexes,[21–24] alkylthiolate-ligated **4** is capable of abstracting H atoms from strong C–H bonds, on par with that of the β C–H bonds of cysteine (93 kcal/mol).[33] It is plausible that π-back-donation by the electron-rich alkyl thiolate facilitates this reactivity by increasing the basicity of the distal oxygen. Spectroscopic characterization of **4**, along with calibrated DFT calculations, provides additional evidence to support the assignment of the IPNS and CDO intermediates detected via transient absorption spectroscopy,[2,5] as *cis* RS-Fe^{III}-$O_2^{\bullet-}$ species.

Supplementary Material

Refer to Web version on PubMed Central for supplementary material.

ACKNOWLEDGMENTS

Funding from the NIH (RO1-GM123062) is gratefully acknowledged. We thank Elizabeth Canarie and Donald Mannikko for assistance with EPR spin quantitation.

REFERENCES

(1). Burzlaff NI; Rutledge PJ; Clifton IJ; Hensgens CMH; Pickford M; Adlington RM; Roach PL; Baldwin JE The reaction cycle of isopenicillin N synthase observed by X-ray diffraction. Nature 1999, 401, 721–724. [PubMed: 10537113]

(2). Tamanaha EY; Zhang B; Guo Y; Chang W-C; Barr EW; Xing G; St. Clair J; Ye S; Neese F; Bollinger JM Jr; Krebs C Spectroscopic evidence for the two C-H-cleaving intermediates of Aspergillus nidulans isopenicillin N synthase. J. Am. Chem. Soc. 2016, 138, 8862–8874. [PubMed: 27193226]

(3). Roach PL; Clifton IJ; Hensgens CMH; Shibata N; Schofield CJ; Hajdu J; Baldwin JE Structure of isopenicillin N synthase complexed with substrate and the mechanism of penicillin formation. Nature 1997, 387, 827–830. [PubMed: 9194566]

(4). Brown CD; Neidig ML; Neibergall MB; Lipscomb JD; Solomon EI VTVH-MCD and DFT Studies of Thiolate Bonding to $\{FeNO\}^7/\{FeO_2\}^8$ Complexes of Isopenicillin N Synthase: Substrate Determination of Oxidase versus Oxygenase Activity in Nonheme Fe Enzymes. J. Am. Chem. Soc. 2007, 129 (23), 7427–7438. [PubMed: 17506560]

(5). Tchesnokov EP; Faponle AS; Davies CG; Quesne MG; Turner R; Fellner M; Souness RJ; Wilbanks SM; deVisser SP; Jameson GNL An iron–oxygen intermediate formed during the catalytic cycle of cysteine dioxygenase. Chem. Commun. 2016, 52, 8814–8817.

(6). Kumar D; Thiel W; de Visser SP Theoretical Study on the Mechanism of the Oxygen Activation Process in Cysteine Dioxygenase Enzymes. J. Am. Chem. Soc. 2011, 133, 3869–3882. [PubMed: 21344861]

(7). Crawford JA; Li W; Pierce BS Single Turnover of Substrate-Bound Ferric Cysteine Dioxygenase with Superoxide Anion: Enzymatic Reactivation, Product Formation, and a Transient Intermediate. Biochemistry 2011, 50, 10241–10253. [PubMed: 21992268]

(8). Aluri S; de Visser SP The Mechanism of Cysteine Oxygenation by Cysteine Dioxygenase Enzymes. J. Am. Chem. Soc. 2007, 129, 14846–14847. [PubMed: 17994747]

(9). Joseph CA; Maroney MJ Cysteine dioxygenase: structure and mechanism. Chem. Commun. 2007, 3338–3349.

(10). Pierce BS; Gardner JD; Bailey LJ; Brunold TC; Fox BG Characterization of the nitrosyl adduct of substrate-bound mouse cysteine dioxygenase by electron paramagnetic resonance: electronic structure of the active site and mechanistic implications. Biochemistry 2007, 46, 8569–8578. [PubMed: 17602574]

(11). Kovacs JA How Iron Activates O2. Science 2003, 299, 1024–1025. [PubMed: 12586930]

(12). Kennepohl P; Neese F; Schweitzer D; Jackson HL; Kovacs JA; Solomon EI Spectroscopy of Non-Heme Iron Thiolate Complexes: Insight into the Electronic Structure of the Low-Spin Active Site of Nitrile Hydratase. Inorg. Chem. 2005, 44, 1826–1836. [PubMed: 15762709]

(13). Kovacs JA; Brines LM Understanding How the Thiolate Sulfur Contributes to the Function of the Non-Heme Iron Enzyme Superoxide Reductase. Acc. Chem. Res. 2007, 40 (7), 501–9. [PubMed: 17536780]

(14). Villar-Acevedo G; Nam E; Fitch S; Benedict J; Freudenthal J; Kaminsky W; Kovacs JA Influence of Thiolate Ligands on Reductive N–O Bond Activation. Oxidative Addition of NO to a Biomimetic SOR Analogue, and its Proton-Dependent Reduction of Nitrite. J. Am. Chem. Soc. 2011, 133, 1419–1427. [PubMed: 21207999]

(15). Yosca TH; Rittle J; Krest CM; Onderko EL; Silakov A; Calixto JC; Behan RK; Green MT Iron(IV)hydroxide pKa and the Role of Thiolate Ligation in C–H Bond Activation by Cytochrome P450. Science 2013, 342, 825–829. [PubMed: 24233717]

(16). Green MT C–H bond activation in heme proteins: the role of thiolate ligation in cytochrome P450. Curr. Opin. Chem. Biol. 2009, 13, 84–88. [PubMed: 19345605]

(17). Heafield MT; Fearn S; Steventon GB; Waring RH; Williams AC; Sturman SG Plasma cysteine and sulphate levels in patients with motor neurone, Parkinson's and Alzheimer's disease. Neurosci. Lett. 1990, 110, 216–220. [PubMed: 2325885]

(18). Dietrich D; Krispin M; Dietrich J; Fassbender A; Lewin J; Harbeck N; Schmitt M; Eppenberger-Castori S; Vuaroqueaux V; Spyratos F; Foekens JA; Lesche R; Martens JWM CDO1 promoter methylation is a biomarker for outcome prediction of anthracycline treated, estrogen receptor-positive, lymph node-positive breast cancer patients. BMC Cancer 2010, 10, 247. [PubMed: 20515469]

(19). Jeschke J; O'Hagan HM; Zhang W; Vatapalli R; Freitas Calmon M; Danilova L; Nelkenbrecher C; Van Neste L; Bijsmans ITGW; Van Engeland M; Gabrielson E; Schuebel KE; Winterpacht A; Baylin SB; Herman JG; Ahuja N Frequent Inactivation of Cysteine Dioxygenase Type 1 Contributes to Survival of Breast Cancer Cells and Resistance to Anthracyclines. Clin. Cancer Res. 2013, 19, 3201–3211. [PubMed: 23630167]

(20). Rauk A; Yu D; Armstrong DA Oxidative Damage to and by Cysteine in Proteins: An ab Initio Study of the Radical Structures, C-H, S-H, and C-C Bond Dissociation Energies, and Transition Structures for H Abstraction by Thiyl Radicals. J. Am. Chem. Soc. 1998, 120, 8848–8855.

(21). Hong S; Sutherlin KD; Park J; Kwon E; Siegler MA; Solomon EI; Nam W Crystallographic and spectroscopic characterization and reactivities of a mononuclear non-haem iron-(III)-superoxo complex. Nat. Commun. 2014, 5, 5440–5447. [PubMed: 25510711]

(22). Chiang C-W; Kleespies ST; Stout HD; Meier KK; Li P-Y; Bominaar EL; Que L Jr.; Munck E; Lee W-Z Characterization of a Paramagnetic Mononuclear Nonheme Iron-Superoxo Complex. J. Am. Chem. Soc. 2014, 136, 10846–10849. [PubMed: 25036460]

(23). Fischer AA; Lindeman SV; Fiedler AT A synthetic model of the nonheme iron–superoxo intermediate of cysteine dioxygenase. Chem. Commun. 2018, 54, 11344–11347.

(24). Oddon F; Chiba Y; Nakazawa J; Ohta T; Ogura T; Hikichi S Characterization of Mononuclear Non-heme Iron(III)-Superoxo Complex with a Five-Azole Ligand Set. Angew. Chem., Int. Ed. 2015, 54, 7336–7339.

(25). Krest CM; Silakov A; Rittle J; Yosca TH; Onderko EL; Calixto JC; Green MT Significantly shorter Fe–S bond in cytochrome P450-I is consistent with greater reactivity relative to chloroperoxidase. Nat. Chem. 2015, 7, 696–702. [PubMed: 26291940]

(26). Blaesi EJ; Gardner JD; Fox BG; Brunold TC Spectroscopic and Computational Characterization of the NO Adduct of Substrate-Bound Fe(II) Cysteine Dioxygenase: Insights into the Mechanism of O2 Activation. Biochemistry 2013, 52, 6040–6051. [PubMed: 23906193]

(27). Ellison JJ; Nienstedt A; Shoner SC; Barnhart D; Cowen JA; Kovacs JA Reactivity of Five-Coordinate Models for the Thiolate-Ligated Fe Site of Nitrile Hydratase. J. Am. Chem. Soc. 1998, 120 (23), 5691–5700.

(28). Schweitzer D; Ellison JJ; Shoner SC; Lovell S; Kovacs JA A Synthetic Model for the NO-Inactivated Form of Nitrile Hydratase. J. Am. Chem. Soc. 1998, 120 (42), 10996–10997.

(29). Scarrow RC; Strickler B; Ellison JJ; Shoner SC; Kovacs JA; Cummings JG; Nelson MJ X-Ray Spectroscopy of Nitric Oxide Binding to Iron in Inactive Nitrile Hydratase and a Synthetic Model Compound. J. Am. Chem. Soc. 1998, 120, 9237–9245.

(30). Villar-Acevedo G; Lugo-Mas P; Blakely MN; Rees JA; Ganas AS; Hanada EM; Kaminsky W; Kovacs JA Metal-Assisted Oxo Atom Addition to an Fe(III)-Thiolate. J. Am. Chem. Soc. 2017, 139, 119–129. [PubMed: 28033001]

(31). Shearer J; Jackson HL; Schweitzer D; Rittenberg DK; Leavy TM; Kaminsky W; Scarrow RC; Kovacs JA The first example of a nitrile hydratase model complex that reversibly binds nitriles. J. Am. Chem. Soc. 2002, 124, 11417–11428. [PubMed: 12236756]

(32). Baldwin JE; Abraham E The Biosynthesis of Penicillins and Cephalosporins. Nat. Prod. Rep. 1988, 5, 129–145. [PubMed: 3145474]

(33). Luo Y-R Comprehensive Handbook of Chemical Bond Energies; Taylor and Francis Group: Boca Raton, FL, 2007.

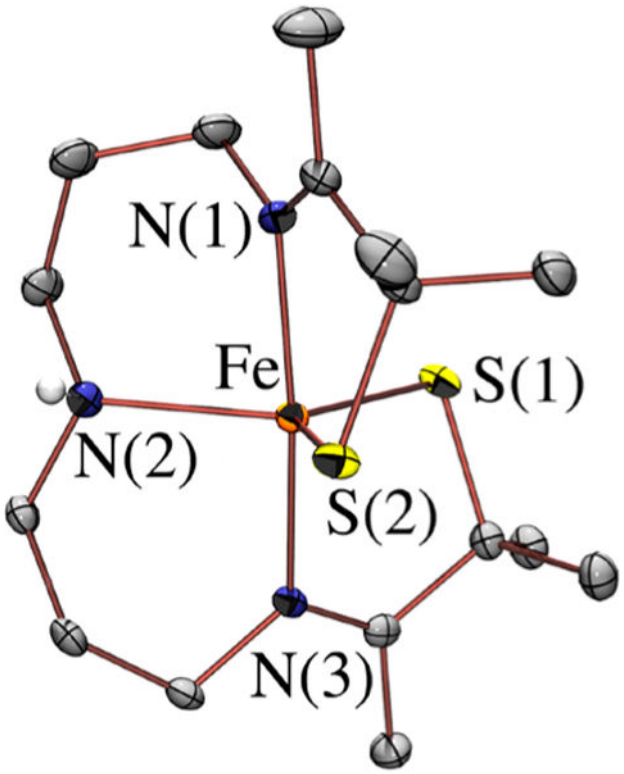

Figure 1.
ORTEP of **1** with thermal ellipsoids at the 50% probability level. With the exception of the secondary amine proton, hydrogens have been removed for clarity.

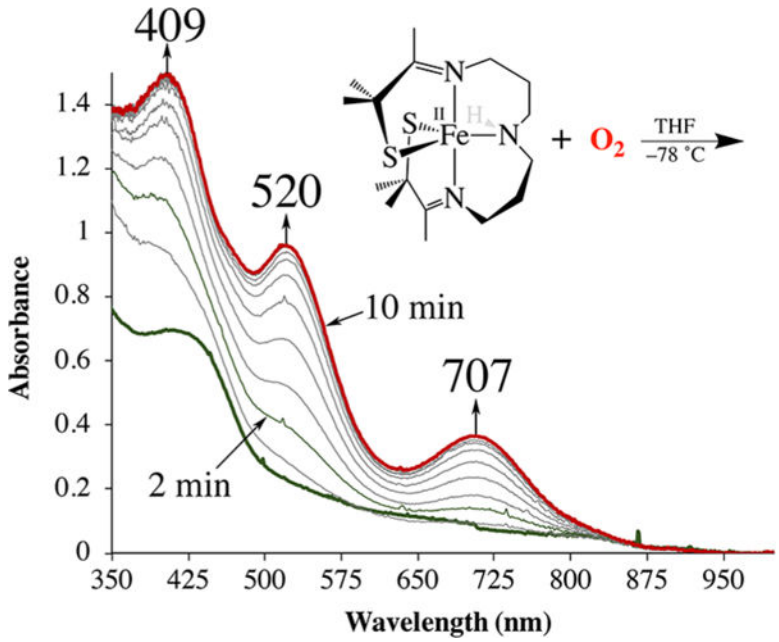

Figure 2.

Monitoring the low temperature (−73 °C) reaction between 1 (0.48 mM) and excess O_2 in THF by electronic absorption spectroscopy.

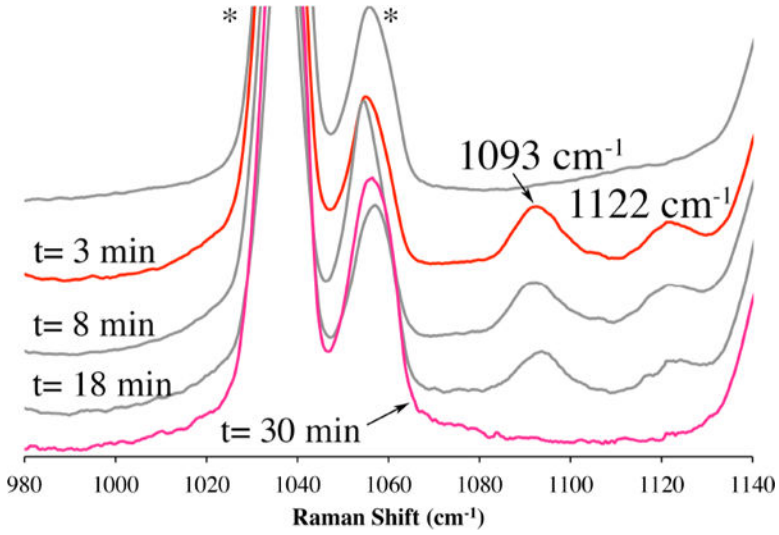

Figure 3.

Monitoring the reaction between **1** (5 mM) and O_2 in THF at −73 °C by resonance Raman spectroscopy. Samples were frozen in liquid N_2 (77 K) at the time-intervals indicated. Excitation wavelength λ_{ex} = 527 nm; 4.0 mW power; * = solvent peak.

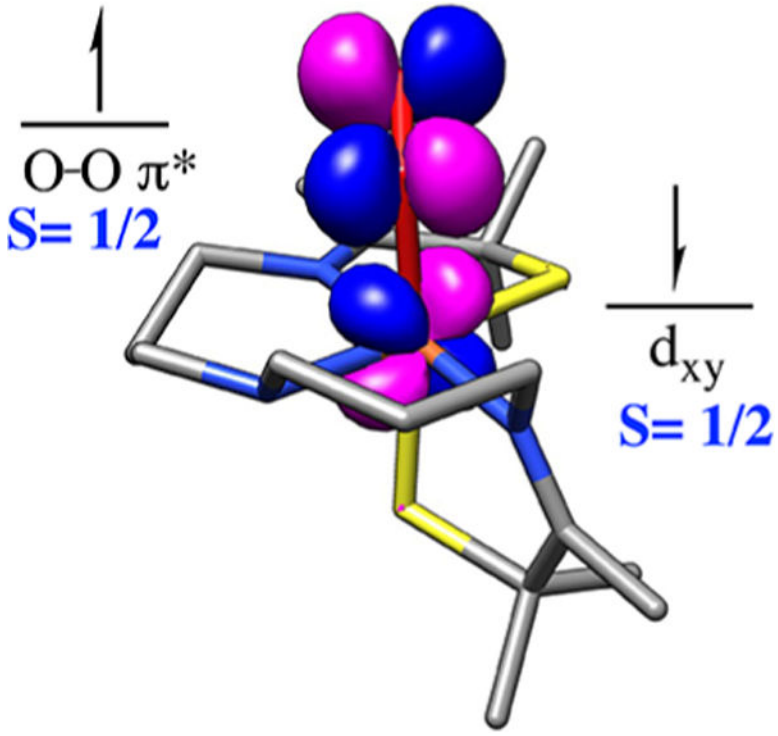

Figure 4.

Singly occupied molecular orbitals (SOMO) of **4** contain strongly coupled electrons of opposite spin, one on the superoxo ($O_2^{\bullet -}$) and the other on the metal ion.

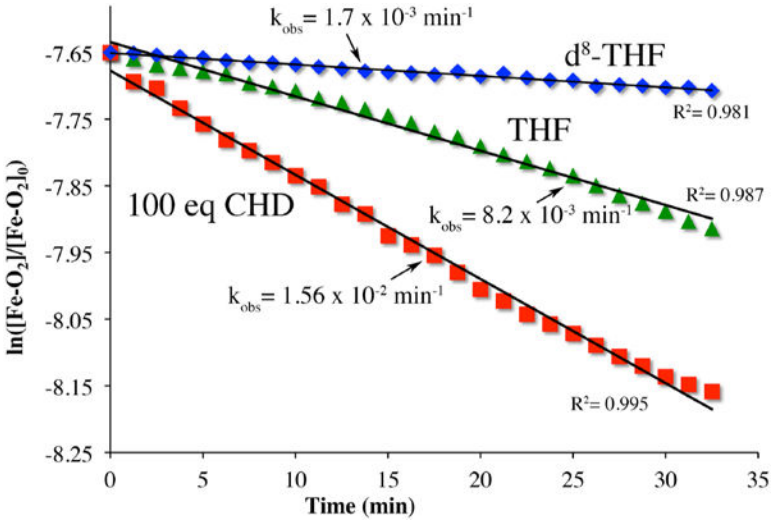

Figure 5.

Pseudo-first-order kinetic plots associated with the reaction between **4** (0.48 mM) and THF (12 M), or CHD (48 mM) in THF at −73 °C.

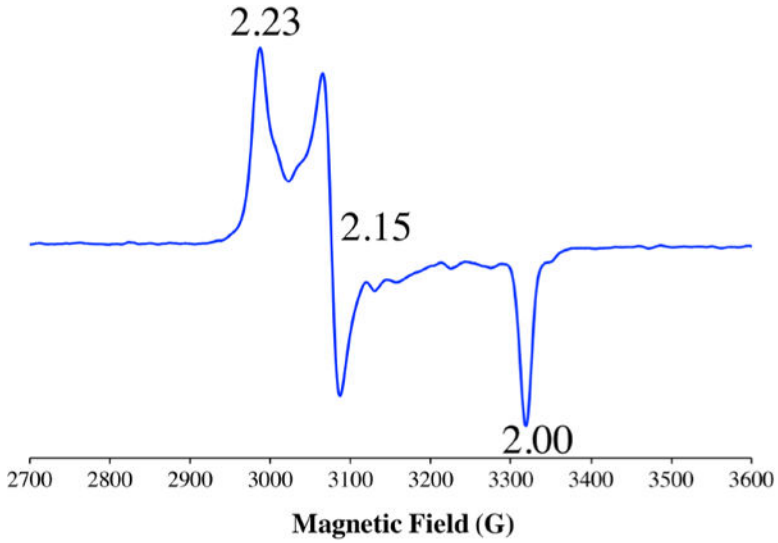

Figure 6.

X-band EPR spectrum (⊥-mode) of putative hydroperoxo Fe^{III}–OOH (**5**), formed from superoxo Fe^{III}–$O_2^{\bullet-}$ (**4**) via H atom abstraction.